Journal of Hydrology 519 (2014) 2289–2300

Contents lists available at ScienceDirect

Journal of Hydrology

journal homepage: www.elsevier.com/locate/jhydrol

Application of the water table fluctuation method for estimating evapotranspiration at two phreatophyte-dominated sites under hyper-arid environments

Ping Wang [a,c,d], Sergey O. Grinevsky [b], Sergey P. Pozdniakov [b], Jingjie Yu [a,*], Dina S. Dautova [b], Leilei Min [a,e], Chaoyang Du [a,f], Yichi Zhang [a]

[a] Key Laboratory of Water Cycle & Related Land Surface Processes, Institute of Geographic Sciences and Natural Resources Research, Chinese Academy of Sciences, 11A, Datun Road, Chaoyang District, Beijing 100101, China
[b] Department of Hydrogeology, Moscow State University, GSP-1, Leninskie Gory, Moscow 119899, Russia
[c] Biosphere 2, University of Arizona, 32540 S Biosphere Rd, Oracle, Tucson, AZ 85739, USA
[d] Department of Hydrology and Water Resources, University of Arizona, 1133 E James E Rogers Way, Tucson, AZ 85721, USA
[e] Key Laboratory of Agricultural Water Resources, Center for Agricultural Resources Research, Chinese Academy of Sciences, Shijiazhuang 050021, China
[f] University of Chinese Academy of Sciences, 19A, Yuquan Road, Beijing 100049, China

ARTICLE INFO

Article history:
Received 26 June 2014
Received in revised form 30 August 2014
Accepted 30 September 2014
Available online 8 October 2014
This manuscript was handled by Corrado Corradini, Editor-in-Chief, with the assistance of Renduo Zhang, Associate Editor

Keywords:
Evapotranspiration
Water table fluctuation
Phreatophyte
Arid area
Heihe River Basin

SUMMARY

Shallow groundwater is primarily discharged via evapotranspiration (ET_g) in arid and semi-arid riparian systems; however, the quantification of ET_g remains a challenge in regional water resource assessments of such systems. In this study, the diagnostic indicators of groundwater evapotranspiration processes and the principles of applying the water table fluctuation (WTF) method to estimate ET_g based on seasonal groundwater level changes were presented. These techniques were then used to investigate groundwater evapotranspiration processes at two sites dominated by phreatophytes (*Tamarix ramosissima* and *Populus euphratica*) within hyper-arid desert environments in northwestern China for the period 2010–2012. The results indicate that steady declines in the water table, which are commonly attributed to groundwater evapotranspiration, occurred at both sites during the growing season. Based on the proposed WTF method, the estimated ET_g was 0.63–0.73 mm/d at the *Tamarix ramosissima* site and 1.89–2.33 mm/d at the *Populus euphratica* site during the summer months (June–August). Numerical simulations using a one-dimensional root water uptake model indicate that the seasonal variations in ET_g at both sites were primarily dependent on the potential evaporation rates. Comparisons with previous studies on plant transpiration at similar sites in this area show that these results are reasonable. It is apparent that the WTF method can provide a simple and relatively inexpensive method of estimating ET_g on a large scale in arid/semi-arid regions. However, there are significant uncertainties associated with time-dependent lateral flow rates, which creates a challenge when applying this method. In addition, the selection of calculation periods that show steady declines in the groundwater level can be somewhat subjective. To enhance the performance of the WTF method based on seasonal water table declines, further research on the estimation of lateral flow rates should be performed using an effective network of groundwater monitoring.

© 2014 Elsevier B.V. All rights reserved.

1. Introduction

Evapotranspiration from the land surface is the process through which water is transferred from a liquid (or ice) phase to the vapor phase, which includes plant transpiration through leaf stomata and evaporation from soil, wet leaves and water bodies (Lautz, 2008; Wang and Dickinson, 2012). In arid regions with a relatively shallow groundwater table, groundwater evapotranspiration (ET_g) is a predominant mechanism of groundwater discharge (Nichols, 1994). This process leads to a decline in the groundwater table, an increase in groundwater salinity, and, consequently, deterioration of the ecosystem (Jolly et al., 2008). Therefore, the quantification of ET_g rates, particularly in arid regions where the recharge is small, is a prerequisite for sustainable groundwater resource use and management (Goodrich et al., 2000) as well as natural ecosystem protection and restoration (Drexler et al., 2004). This quantification is particularly important in regions with groundwater-dependent

* Corresponding author.
E-mail address: yujj@igsnrr.ac.cn (J. Yu).

http://dx.doi.org/10.1016/j.jhydrol.2014.09.087
0022-1694/© 2014 Elsevier B.V. All rights reserved.

ecosystems, where all or part of the water demand is supplied by groundwater (Cooper et al., 2006; Naumburg et al., 2005; Orellana et al., 2012; Yuan et al., 2014). However, the accurate estimation of ET_g remains a challenge in that it is typically subject to uncertainties associated with climatic variables, vegetation parameters, geological variables, and hydrologic parameters (Gou and Miller, 2014; Newman et al., 2006).

Diurnal and seasonal trends in groundwater levels across large areas provide the basic information required to understand natural and human-induced processes such as groundwater recharge and discharge in the hydrologic system (Alley et al., 2002; Woessner, 2000). It is well known that seasonal fluctuations in the groundwater table can often be identified as a result of the seasonality of evapotranspiration in arid and semi-arid areas (Healy and Cook, 2002). In addition, diurnal fluctuations in the groundwater table have been widely observed in riparian areas in response to phreatophyte uptake of groundwater via evapotranspiration (Gribovszki et al., 2013; Ridolfi et al., 2007; White, 1932). The development of electronic pressure transducers and digital data recorders has recently made high-frequency groundwater level monitoring possible and provided abundant opportunities for using this type of information (Freeman et al., 2004; Gribovszki et al., 2010). The water table fluctuation (WTF) method, which is based on the premise that changes in the water table in unconfined aquifers are caused by evapotranspiration (Healy and Cook, 2002; Lautz, 2008), has been widely used to estimate ET_g rates in riparian zones in arid and semi-arid areas (e.g., Carlson Mazur et al., 2014; Gribovszki et al., 2008; Soylu et al., 2012; Weeks and Sorey, 1973; Yin et al., 2013; Zhu et al., 2011).

In this study, the patterns of daily and seasonal groundwater fluctuations in a desert environment in northwestern China with scant precipitation (less than 50 mm per year) and strong potential evapotranspiration (more than 1400 mm per year) were analyzed. We used the WTF approach to estimate ET_g at two typical phreatophyte-dominated sites (*Tamarix ramosissima* and *Populus euphratica*) in this area. The primary objectives of this study were to (i) characterize the seasonal and diurnal groundwater dynamics and analyze their controlling factors; (ii) quantify the ET_g rate using the WTF method and evaluate its seasonal patterns using a 1-D root water uptake model; and (iii) examine the relationships between the ET_g rates and corresponding values of E-601 pan evaporation (E_{601}) during multiple growing seasons.

2. Theoretical background

It is assumed that fluctuations in the depth to the water table (Z_g) in areas with groundwater ET can be viewed as a superposition of seasonal trends (Z_s), daily harmonic-like fluctuations (Z_d), and residuals (Z_r) (Wang and Pozdniakov, 2014):

$$Z_g = Z_s + Z_d + Z_r. \tag{1}$$

The WTF method, which is predominantly based on the analysis of seasonal trends in groundwater table hydrographs $H(t)$, is typically used to quantify groundwater recharge/discharge rates (Healy and Cook, 2002; Nimmo et al., 2014; Sophocleous, 1991; Varni et al., 2013). The decision to apply the WTF method to estimate ET_g in arid and semi-arid areas is primarily based on the following assumptions (Healy, 2010; Weeks and Sorey, 1973): (1) seasonal scaled declines in groundwater levels, $\Delta H = -\Delta Z_s$, which are primarily affected by ET_g, are relatively stable during the growing season; (2) the lateral flow-induced groundwater recharge/discharge rate in a near-well region does not change over the entire growing season; and (3) the value of the specific yield is representative of the selected area. Under the above conditions and using the Dupuit assumption for groundwater flow, the transient planar flow model can be written as follows:

$$\begin{aligned} &-\nabla q_{lat} + ET_g = S_y \frac{\partial H}{\partial t}, \\ &q_{lat} = -T\nabla_{x,y} H, \end{aligned} \tag{2}$$

where S_y is the specific yield [–], T is the transmissivity of groundwater flow [$L^2\,T^{-1}$], q_{lat} is the lateral groundwater flow rate per unit width [$L^2\,T^{-1}$], and H is the groundwater level [L].

Suppose the total change in groundwater level, ΔH, during the growing period can be divided into two components (Fig. 1) in which $\Delta h(x, y, t)$ is the change in groundwater level induced by lateral flow divergence due to far-field (regional) flow conditions and $\Delta z(z, t)$ is the change in groundwater level caused by local seasonal evapotranspiration ET_g, then by substituting h and z into Eq. (2), we obtain the following:

$$-\nabla q_{lat} + ET_g = S_y \frac{\partial (h+z)}{\partial t}. \tag{3}$$

According to our assumption, a change in h does not depend on the local recharge/discharge conditions; therefore, we can treat these changes as being caused by unknown lateral boundary conditions. Therefore, the flow equation for h can be written as follows:

$$-\nabla q_{lat} = S_y \frac{\partial h}{\partial t}. \tag{4}$$

Thus,

$$ET_g = S_y \frac{\partial z}{\partial t}. \tag{5}$$

From Eqs. (3)–(5), ET_g can be calculated for a finite seasonal interval Δt using the following formula:

$$ET_g = S_y \frac{\Delta H - \Delta h}{\Delta t}. \tag{6}$$

The application of Eq. (6) to the estimation of ET_g is restricted by the correct determination of the lateral flow-induced water table change rate $\Delta h/\Delta t$, which is assumed to be independent of evapotranspiration processes. The validity of the estimated value of $\Delta h/\Delta t$ can be confirmed by the identity of $\Delta h/\Delta t$ before and after the growing season (Fig. 1).

A key uncertainty in the WTF method, as mentioned by Healy and Cook (2002) and Lautz (2008), results from the difficulties in estimating the specific yield, which depends on the soil texture, initial water table depth, and rate of change in the water table (Duke, 1972; Nachabe, 2002). To evaluate these dynamics of the

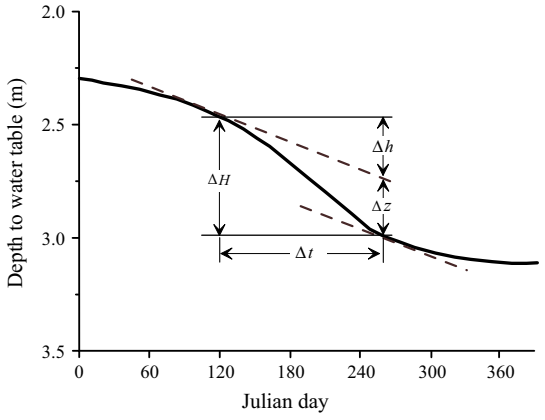

Fig. 1. Schema for calculating seasonal evapotranspiration from a well hydrograph. ΔH is the total change in the groundwater level over Δt, Δh is the change in the groundwater level that is induced by lateral flow divergence due to far-field (regional) flow conditions over Δt, and Δz is the change in the groundwater level that is caused by local seasonal evapotranspiration over Δt.

specific yield, Crosbie et al. (2005) introduced the apparent specific yield (S_y). This parameter is based on the *van Genuchten* model parameters:

$$S_y = S_{yu} - \frac{S_{yu}}{\left[1 + \left(\alpha\left(\frac{z_i + z_f}{2}\right)\right)^n\right]^{1-\frac{1}{n}}}, \quad S_{yu} = \theta_s - \theta_r, \tag{7}$$

where θ_s is the saturated moisture content [$L^3\ L^{-3}$], θ_r is the residual moisture content [$L^3\ L^{-3}$], z_i is the initial depth to water table [L], z_f is the final depth to water table [L], and α and n are parameters of the *van Genuchten* model. When the groundwater table fluctuates in m soil layers, the average apparent specific yield $\overline{S_y}$ can be calculated using the following formula:

$$\overline{S_y} = \frac{\sum_{i=1}^{m} \Delta h_i S_{y_i}}{\sum_{i=1}^{m} \Delta h_i}, \quad i = 1, 2, \ldots, m, \tag{8}$$

where Δh_i is the amplitude of the groundwater level change in the i soil layer [L], and S_{y_i} is the specific yield of the corresponding soil layer [–].

Despite the above-mentioned limitations, the WTF method remains one of the most widely used approaches for estimating the seasonal ET_g, particularly in arid and semi-arid environments. One of the advantages of this method lies in its simplicity and limited data requirements: records of groundwater level and estimates of specific yield. Compared with the method based on soil moisture balance and energy balance (e.g., Bowen ratio method), estimates of the ET_g using the WTF method are representative of areas of several or, in some cases, thousands of square meters (Healy, 2010).

3. Study area and experiment

3.1. Overview of study area

The Ejina Oasis (100°10′–101°20′E and 41°00′–42°40′N), which is located in the lower reaches of the Heihe River Basin (Fig. 2), is the second largest inland river in northwestern China and is characterized by a hyper-arid environment with extremely hot summers and severely cold winters. Based on data collected at the Ejina weather station (Fig. 2) from 1960 to 2012, the mean annual air temperature is 8.96 °C, with a maximum monthly mean air temperature of 27.0 °C in July and a minimum of −11.5 °C in January (Fig. 3). The average annual precipitation is approximately

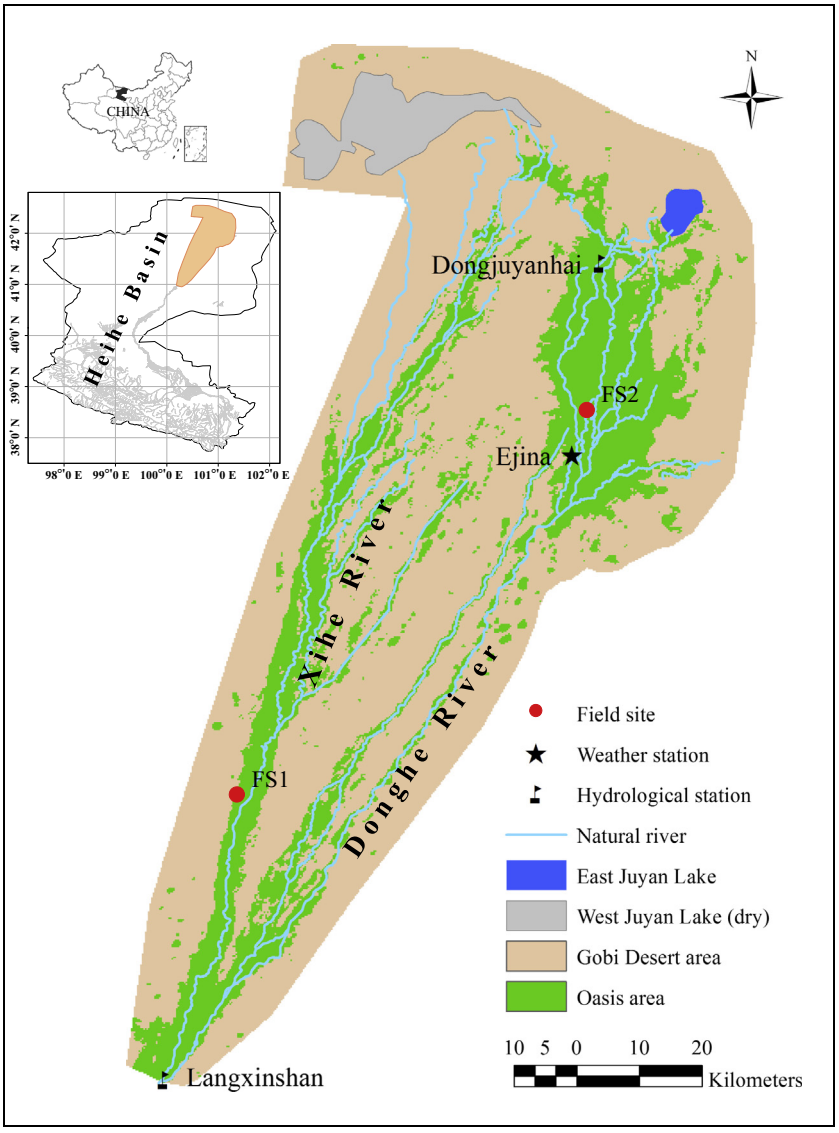

Fig. 2. The study area and locations of the two field sites FS1 and FS2. The spatial distributions of the Gobi Desert and oases were modified from Zhang et al. (2011).

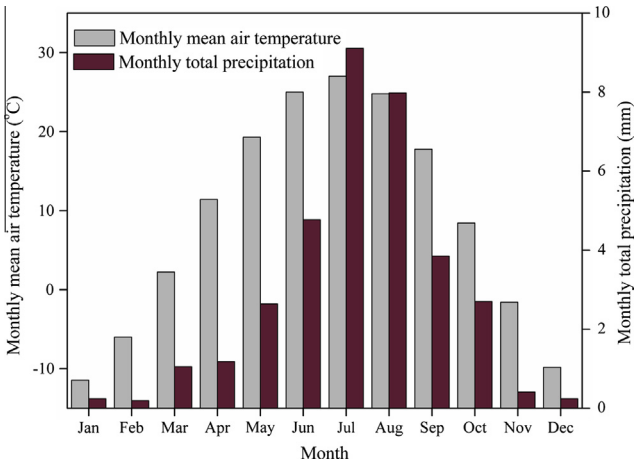

Fig. 3. Monthly mean air temperatures and precipitation at the Ejina weather station from 1960 to 2012; the location of the weather station is shown in Fig. 2.

34.3 mm. The rainfall is highly seasonal; approximately 75% of the total precipitation falls during the months of June–September (Fig. 3). The average annual potential evapotranspiration during the same period is estimated at approximately 1410 mm, which is 40 times greater than the average annual precipitation (Wang et al., 2014).

The lower Heihe River, which is divided into two losing streams in Langxinshan (Donghe and Xihe Rivers), flows through the Ejina Oasis before entering terminal lakes (East and West Juyan Lakes) (Fig. 2). These river systems are the primary source of shallow groundwater recharge via riverbed infiltration (Qin et al., 2012; Wang et al., 2014) due to relatively high vertical hydraulic conductivity (Min et al., 2013). Approximately 71.5% of the landscape in this area is represented by the Gobi desert (Zhang et al., 2011), which consists of wind-eroded hilly areas, desert, and alkaline soils (Xie, 1980). The other 28.5% of the land area is characterized by natural oasis ecosystems that consist of two vegetation zones distributed along the Donghe and Xihe Rivers and their distributaries (Zhang et al., 2011) (Fig. 2). The predominant natural vegetation, which is characterized by phreatophytes (e.g., *Populus euphratica* and *Tamarix ramosissima*), relies primarily on groundwater for survival (Wang et al., 2011b; Si et al., 2014). Detailed descriptions of the study area were presented by Qin et al. (2012) and Wang et al. (2014).

3.2. Experimental sites

Previous studies (Wang et al., 2013, 2014; Wen et al., 2005) have indicated that evapotranspiration is the predominant mechanism of groundwater discharge from the shallow, unconfined aquifer of the Ejina Oasis, where the depth to water table typically varies between 2 and 4 m (Wang et al., 2011a). In this work, two field sites were selected to investigate the seasonal ET_g rate and its response to the most important aspects of the environment, including the climate, types of vegetation, soil, and depth to groundwater table.

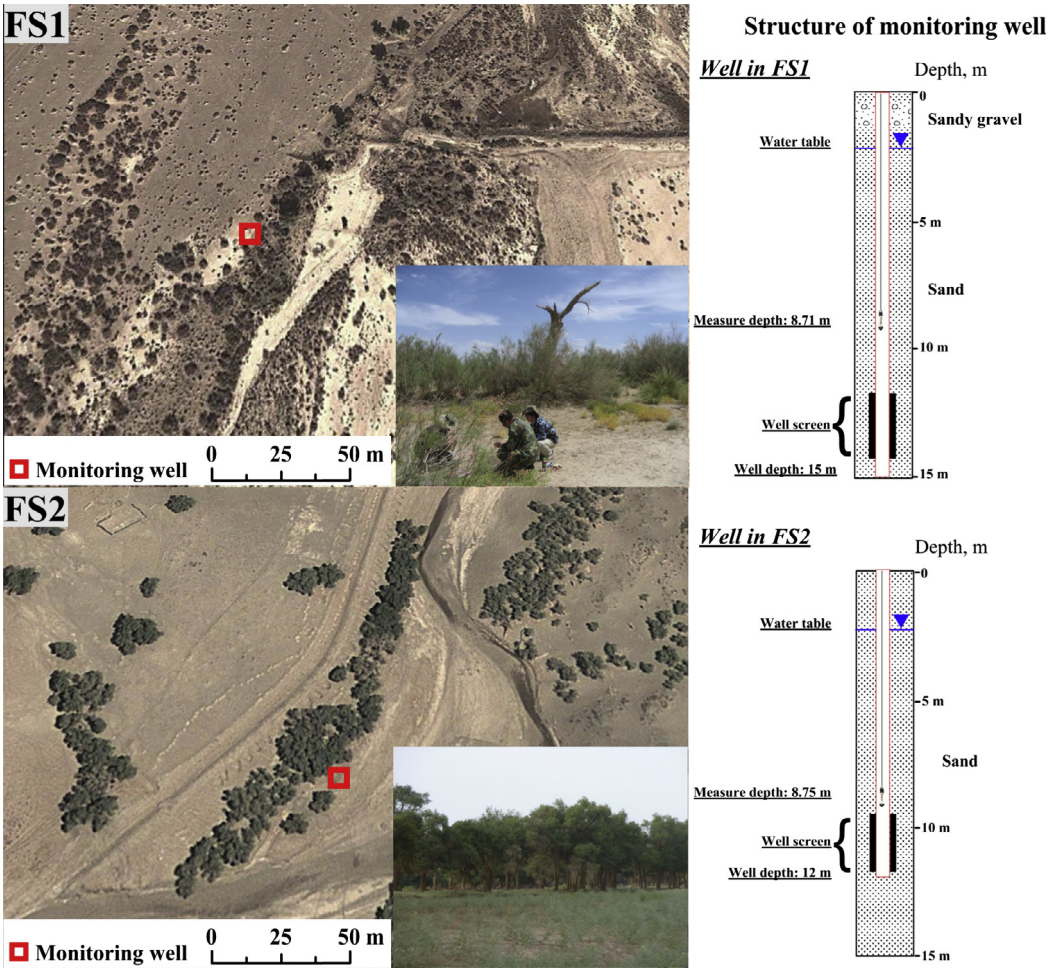

Fig. 4. Typical landscapes (left) and the monitoring well designs (right) used at field sites FS1 and FS2.

3.2.1. Vegetation characterization

As shown in Fig. 2, site FS1 (shrub land) is located on the beach of the upper Xihe River; the distance to the riverbank is approximately 2000 m. The plant community at this site is dominated by *Tamarix ramosissima*, a shrub commonly found in this region. A small collection of the companion species *Artemisia* sp. and *Sophora alopecuroides* is distributed across this shrub land (Fig. 4). The total plant coverage is estimated at approximately 60% (Zhu et al., 2012). The major soil types include sandy soil, meadow soil, and gray brown desert soil. Site FS2 (wood land) is located in the riparian zone of the distributaries of the lower Donghe River; the site is 15 m from the riverbank (Fig. 2). A strip of *Populus euphratica* forest is present at this site, and a small assortment of herb species such as *Sophora alopecuroides* grow near the ground of the forest (Fig. 4). This site possesses relatively high vegetation densities with a community coverage of approximately 65% (Zhu et al., 2012). Dune formations and a considerable amount of eolian sand have been identified beneath the forest cover.

The Normalized Difference Vegetation Index (NDVI) obtained through remote sensing techniques has been widely used to investigate the fractional vegetation cover and its seasonal and annual dynamics, particularly in arid and semi-arid areas (Jarlan et al., 2008; Mangiarotti et al., 2012; McGwire et al., 2000; Törnros and Menzel, 2014). NDVI time series at the two field sites spanning the period 2010–2012 were obtained from the Moderate Resolution Imaging Spectroradiometer (MODIS) sensors on the Terra satellite. The MODIS NDVI data were supplied by the NASA EROS Data Center as radiometrically and geometrically corrected values representing the best scenes during each 16-day period at resolutions of 250–1000 m (Huete et al., 2002). Fig. 5 shows the temporal variations in the 250-m NDVI at 16-day intervals during the study period at the two field sites. The NDVI data exhibited a sinusoidal pattern at both of the field sites and reached peaks during July of each year.

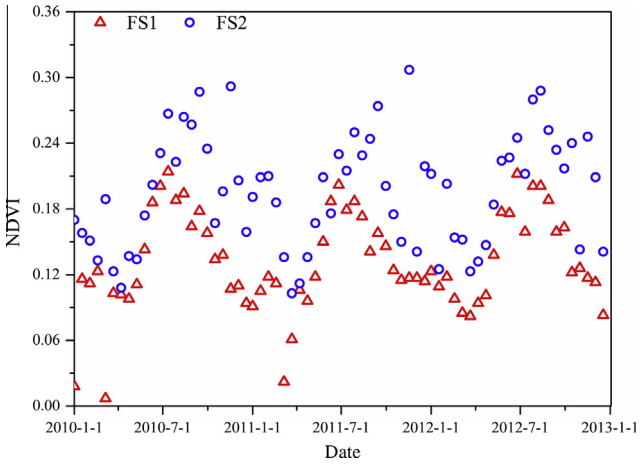

Fig. 5. Temporal variations in the NDVI from 2010 to 2012 at field sites FS1 and FS2.

3.2.2. Soil properties

Extensive analysis of soil textures and their basic physical properties was performed on core samples collected at the two sites during a field soil investigation. Laboratory analyses of the particle size distributions of the samples were performed via sieve analysis (>2-mm fraction) and laser particle size analysis (Malvern Mastersizer 2000 laser diffractometer for the <2-mm fraction). The soil water retention curves for the selected samples were obtained using a Hitachi CR21GIII centrifuge. The aforementioned analyses were performed at the Physical and Chemical Analysis Laboratory of the Institute of Geographic Sciences and Natural Resources Research, Chinese Academy of Sciences, Beijing.

At the shrub site (site FS1), the soil in the vadose zone consists of nearly 100% sand and gravel (Table 1). The soil in the upper layer (0–0.3 m) consists of 77% sand, 19% gravel with a diameter of 2–3 mm, and less than 5% silt. The soil of the underlying layer (0.3–1.7 m) contains a greater proportion of gravel, with a diameter of up to 30 mm (57%), and the rest consists of sand (43%). The lower soil layer (1.7–2.5 m) in the vadose zone consists predominantly of sand. The bulk density of the uppermost layer is 1.72 g/cm^3 and that of the third layer is 1.48 g/cm^3. The hydraulic conductivity of the soil is estimated at 250 cm/d and 367 cm/d in the upper and third layers, respectively (Table 1).

The woodland site (site FS2) is located in a sandy river riparian zone, and the soil profile of the vadose zone there may be divided into three layers (Table 1). The bulk density of the soil varies from 1.49 g/cm^3 to 1.55 g/cm^3 across the three layers. The hydraulic conductivity of the upper layer (0–1.0 m) is 420 cm/d; this value decreases to 201 cm/d in the middle layer (1.0–1.6 m) and increases to 809 cm/d in the third layer (1.6–2.2 m).

Fig. 6 shows the soil water characteristic curve of soil samples obtained from the two field sites. Based on the soil water retention data, the *van Genuchten* parameters were estimated using the RETC computer program (Table 1) (van Genuchten et al., 1991).

3.2.3. Groundwater levels and river flows

As shown in Fig. 4, a monitoring well with a depth of no more than 15 m was installed in 2001 by the Water Resources Research Institute of the Inner Mongolia Autonomous Region at each of the two field sites to measure groundwater levels (Wang et al., 2014). The pressure heads in the two monitoring wells were recorded at 30-min intervals using Schlumberger Mini-Diver pressure transducers located at a depth of approximately 8.7 m. The resolution of the Mini-Diver measurements was 2 mm with an uncertainty of ±5 mm. The pressure head measurements were corrected for

Table 1
Soil physical properties and parameters of the *van Genuchten's* hydraulic model.

Layer no.	Depth intervals (m)	Soil physical properties					*van Genuchten* parameters			
		Gravel (>2 mm) (%)	Sand (2–0.05 mm) (%)	Silt (0.05–0.002 mm) (%)	Bulk density (g/cm^3)	Hydraulic conductivity (cm/d)	θ_r (–)	θ_s (–)	α (cm^{-1})	n (–)
Site FS1 (shrub land)										
FS1-1	0–0.3	19	77	4	1.72	250	0.023	0.273	0.044	2.10
FS1-2	0.3–1.7	57	43	0	No data	No data	No data			
FS1-3	1.7–2.5	0	100	0	1.48	367	0.028	0.387	0.055	2.66
Site FS2 (wood land)										
FS2-1	0–1.0	0	100	0	1.49	420	0.019	0.350	0.109	2.06
FS2-2	1.0–1.6	0	99	1	1.49	201	0.034	0.390	0.076	2.51
FS2-3	1.6–2.2	0	99	1	1.55	809	0.027	0.382	0.112	2.04

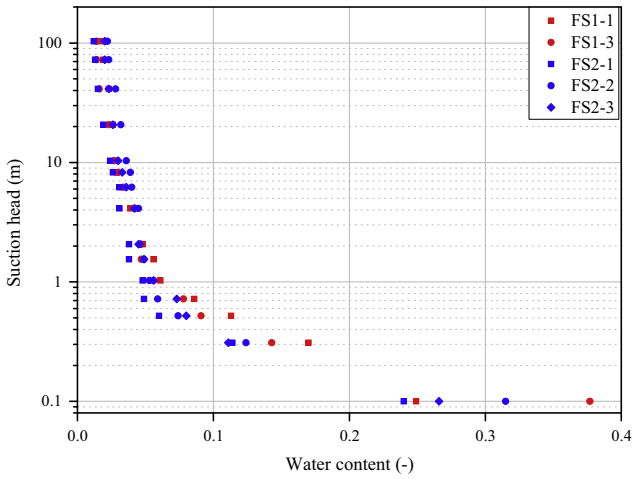

Fig. 6. Soil water characteristic curves for soil samples obtained from field sites FS1 and FS2; the depth intervals of the soil samples are shown in Table 1.

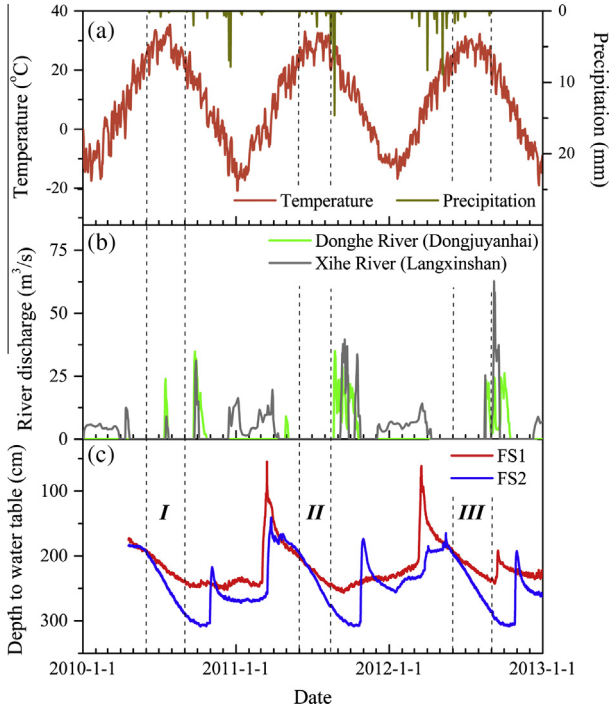

Fig. 7. Daily air temperatures, precipitation, river discharge, and water table fluctuations from 2010 to 2012: (a) air temperature and precipitation; (b) discharge from the Donghe and Xihe Rivers; (c) groundwater level dynamics recorded in wells at field sites FS1 and FS2. Periods *I*, *II*, and *III* exhibit seasonal declines in groundwater levels from June to August.

barometric pressure and Earth tide effects using regression deconvolution calculations, which were performed using the BETCO computer program (Toll and Rasmussen, 2007). Fig. 7c shows the corrected groundwater levels recorded at field sites FS1 and FS2 from 2010 to 2012.

Daily streamflow measurements of the Donghe and Xihe Rivers were performed by the Heihe River Bureau at the Langxinshan and Dongjuyanhai hydrological stations (Fig. 2). Fig. 7b shows the daily streamflow of the Xihe River at the Langxinshan hydrological station (near site FS1) and the daily streamflow of the Donghe River at the Dongjuyanhai hydrological station (near site FS2) (Fig. 2).

4. Results

4.1. Diagnostic indicators of groundwater evapotranspiration

The groundwater levels at sites FS1 and FS2 exhibited notable seasonal variations due to natural patterns of groundwater recharge and discharge (Fig. 7c). Rapid rises in the groundwater table were observed during the spring and autumn due to either riverbed infiltration or direct flood irrigation by river water; however, there was a gradual decline in the groundwater table throughout the summer, which was primarily due to evapotranspiration (Wang et al., 2014). We therefore investigated the ways in which riparian evapotranspiration and groundwater flows generate diurnal fluctuations in water table levels during the vegetation growth season.

Previous studies have documented diurnal fluctuations in groundwater levels in arid and semi-arid areas, which are typically attributed to water losses from evapotranspiration by phreatophytes (Butler et al., 2007; Cheng et al., 2013; Meyboom, 1965). The typical diurnal pattern involves a groundwater table decline during the day due to plant transpiration and groundwater table recovery overnight when transpiration ceases or significantly diminishes (Lautz, 2008; Loheide et al., 2005; White, 1932).

The analysis of the groundwater levels indicates that a diurnal fluctuation with an amplitude of 1–3 cm in the groundwater table occurred from May to September (Wang et al., 2014); however, such fluctuations were practically nonexistent during the winter. As Butler et al. (2007) concluded, diurnal water table fluctuations should be considered an important indicator of groundwater consumption by phreatophytes. To test the hypothesis that groundwater evapotranspiration affects diurnal water table fluctuations, a detrended analysis of a groundwater level time series was performed using the BAYSEA procedure (Akaike, 1980). The temporal variations in the amplitudes of the detrended diurnal groundwater level fluctuations, i.e., Z_d in Eq. (1), can be used to understand the way in which hydrological processes are affected by groundwater evapotranspiration (Wang and Pozdniakov, 2014).

Fig. 8 shows an example of typical Z_d patterns that occurred during the summer (July, 2010), winter (January, 2011), and spring (March, 2011) at site FS1. One can discern a notable diurnal fluctuation in the detrended groundwater level during the summer, with an amplitude of approximately 2 cm; however, such diurnal fluctuations are virtually nonexistent during the winter. Irregular variations in groundwater levels during the winter, which are lower than the measurement uncertainty (±5 mm), are typically attributed to random or systematic errors inherent in the measuring device (Gribovszki et al., 2013; Post and Asmuth, 2013). In contrast to the stable diurnal, detrended groundwater-level fluctuation patterns observed during the summer and winter, a sharp increase and decrease in Z_d can be observed in spring during the period of high river flow, which is clearly related to transient groundwater recharge by river water.

Next, the monthly standard deviation of the diurnal detrended groundwater level fluctuations (σ_d^m) was analyzed. Fig. 8 shows that the σ_d^m increases significantly in May and rises to a maximum in June and July, after which it begins to decease; it then drops significantly by September (Fig. 8). This pattern indicates an increasing amplitude of diurnal fluctuations in the detrended groundwater levels during the summer months. However, σ_d^m remains minimal and nearly unchanged in winter (approximately 0.3 cm at site FS1 site and 0.2 cm at site FS2), which is likely a result of noise in the measurements that are caused by the pressure transducers (Post and Asmuth, 2013). The abnormal σ_d^m that was observed during spring and late autumn can be attributed to the river flow recharge or flooding. Therefore, the analysis of

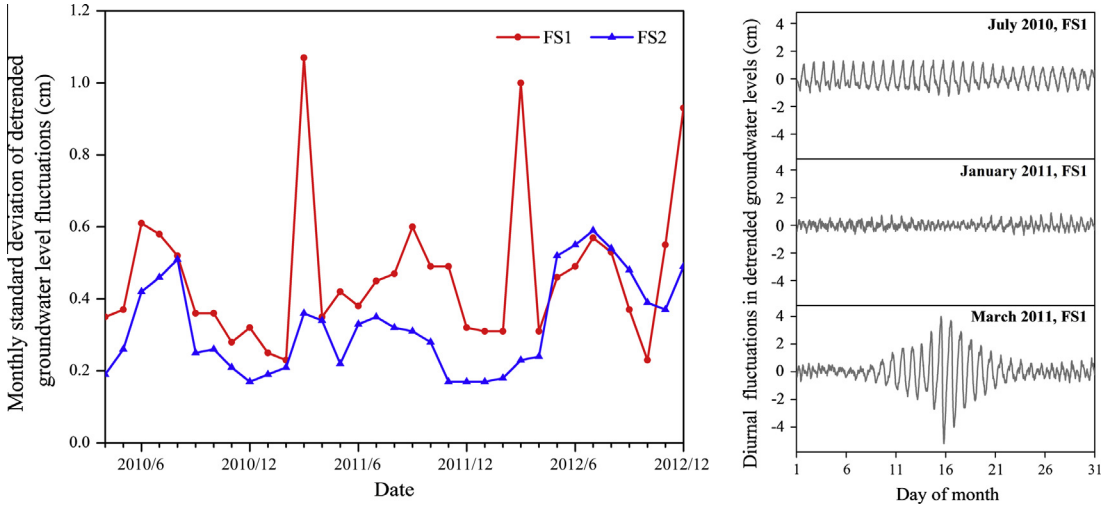

Fig. 8. Monthly standard deviation of detrended groundwater level fluctuations (left) and the typical pattern of diurnal detrended groundwater level fluctuations (right).

diurnal fluctuations in the detrended groundwater levels and their monthly standard deviations indicate that the groundwater evapotranspiration during the summer is the primary cause of the diurnal fluctuations in the detrended groundwater levels and is the cause of its seasonal decline.

4.2. Approximation of evapotranspiration using the WTF method

Three periods during the summer, each spanning 64–99 days (periods I, II, and III in Table 2), were selected to estimate ET_g using the WTF method. As shown in Fig. 7c, distinct declines in the water table were observed at both field sites during these periods. There was no flow in the Xihe River near site FS1 during the selected periods, except for July 18–24, 2010, during which an average discharge of 5.4 m^3/s was recorded at the Langxinshan hydrological station (Fig. 7b). There was also no flow in the distributary of the lower Donghe River near site FS2 during the summer periods. A limited amount of precipitation (up to 26 mm) was observed at the Ejina weather station during each period (Fig. 7a). As shown in Table 2, the average air temperatures ranged from 26.1 °C to 28.2 °C, and the average daily evaporation rate measured using the E-601 pan method (E_{601}) varied from 10.26 mm/d to 11.44 mm/d during the selected periods. The field investigations revealed that there was no pumping from the aquifer within a 5-km radius from both sites. Therefore, the general decline in the water table during the summer months was primarily caused by lateral groundwater discharge and direct water uptake by plant roots.

4.2.1. Determination of the specific yield

The specific yield is a crucial parameter for estimating the water budget components, such as groundwater recharge and evapotranspiration (Chen et al., 2010; Fahle and Dietrich, 2014). Uncertainty in this parameter can contribute the largest errors in estimates of ET_g when using the WTF approach (Shah et al., 2007). Laboratory and field investigations have demonstrated that the specific yield exhibits a high variability depending on the physical characteristics of the soil sediments, temperatures, mineral composition of the water (Johnson, 1967), and different stresses of wetting, drying, pumping, and equilibrium (Shah and Ross, 2009).

During each of the calculation periods, the water table fluctuated within the sandy aquifers at both field sites. The apparent specific yields obtained from Eqs. (7) and (8) were 0.35 and 0.34 at sites FS1 and FS2, respectively. According to similar research conducted by Loheide et al. (2005), the readily available specific yield in sandy sediment was estimated to be 0.32 when the depth to the water table exceeded 1 m. Thus, it is evident that the specific yield estimates for both sites are reasonable.

4.2.2. Estimates of lateral groundwater divergence due to regional flow

Based on the lateral groundwater flow and groundwater evapotranspiration that occurred during the growing season in the absence of river flow, sites FS1 and FS2 are situated in the discharge zone. According to the assumptions of the WTF method that are described in Eqs. (3) and (4), the lateral groundwater flow divergence $-\nabla q_{lat}$ away from the groundwater ET-induced discharge zone is assumed to be constant over the selected time period during each growing season. The value of $-\nabla q_{lat}$ can be estimated using changes in the groundwater level before and after the transpiration season.

As shown in Table 2, the estimated $-\nabla q_{lat}$ during the three periods remained relatively constant (1.26–1.27 mm/d) at site FS1. Slight fluctuations in $-\nabla q_{lat}$ occurred at site FS2, varying from 1.44 mm/d to 1.58 mm/d. The difference in $-\nabla q_{lat}$ between the two sites was related to the differing hydrologic conditions. The

Table 2
Specific yields (S_y), groundwater evapotranspiration rates (ET_g), and additional parameters.

Period	Time span (d)	ΣP (mm)	$\overline{T}$ (°C)	E_{601} (mm/d)	$\overline{z}$ (cm)	ΔH (cm)	Δh (cm)	Δz (cm)	S_y (–)	$-\nabla q_{lat}$ (mm/d)	ET_g (mm/d)	ET_g/E_{601} (–)	$ET_g/\overline{T}$ (mm/(d °C))
Site FS1 (shrub land)													
I (June 7 to August 23, 2010)	78	1.0	28.2	11.44	218	42	28	14	0.35	1.26	0.63	0.055	0.022
II (May 23 to August 7, 2011)	77	9.0	27.4	11.17	221	44	28	16	0.35	1.27	0.73	0.065	0.027
III (May 23 to July 25, 2012)	64	21.6	26.1	10.36	206	35	23	12	0.35	1.26	0.66	0.064	0.025
Site FS2 (wood land)													
I (May 29 to September 4, 2010)	99	1.6	27.5	10.99	243	102	46	56	0.34	1.58	1.92	0.175	0.070
II (June 1 to August 12, 2011)	73	9.1	28.2	11.12	235	81	31	50	0.34	1.44	2.33	0.210	0.083
III (May 29 to September 4, 2012)	99	26.0	26.1	10.26	241	97	42	55	0.34	1.44	1.89	0.184	0.072

monitoring well at site FS1 was located 2000 m from the Xihe River, whereas the monitoring well at site FS2 was located only 15 m from the lower Donghe River distributary.

4.2.3. Groundwater ET estimates

Estimates of ET_g were calculated using the REGIM_3 program (Shtengelov, 2009), which is based on the calculation principle represented in Eq. (6). As shown in Table 2, the estimated ET_g rate at site FS1 during the calculation periods from 2010 to 2012 ranged from 0.63 mm/d to 0.73 mm/d, with an average of 0.67 mm/d. During the same period, the ET_g rate at site FS2 ranged from 1.89 mm/d to 2.33 mm/d; an average was 2.05 mm/d.

Previous studies (Cleverly et al., 2006; Cooper et al., 2006; Devitt et al., 2011) have shown that the climate, vegetation parameters, soil properties, and depth to the water table are the principal factors that control the ET_g in phreatophytic communities. The climate, soil types, and depths to the water table at the two sites are similar, and thus their different ET_g rates are likely due to the differing plant community compositions and plant canopy cover characteristics at the two sites. As shown in Fig. 5, the 3-year average NDVI during the growing season (May–September) was 0.172 at the mixed shrub site (FS1) and 0.228 at the woodland site (FS2). We believe that the significantly higher estimated ET_g rates at the woodland site are directly linked to the specific plant community (i.e., *Populus euphratica*) and the higher percentage of plant canopy cover at this site. However, the slight variations in ET_g rates at each site during the three calculation periods are likely caused by the combined effects of climate variables, water table variations, and vegetation dynamics (Table 2).

4.3. Estimation of temporal variability in groundwater ET using root zone modeling

In Section 4.2.3, the mean ET_g rates during the summer months (June–August) were estimated using the WTF method (Table 2). However, high temporal variations in the ET_g rates that largely depend on complex interactions between the groundwater, soil moisture, vegetation, and the atmosphere were identified (Gou and Miller, 2014; Newman et al., 2006; Orellana et al., 2012). To determine the seasonal variations in the ET_g, the daily ET_g rates were estimated using a saturated–unsaturated flow model.

4.3.1. Model setup

Similar to the approach used by Wang and Pozdniakov (2014), a one-dimensional vertical saturated–unsaturated profile within the groundwater discharge zone caused by evapotranspiration was used to estimate the seasonal dynamics of ET_g. We assumed that the soil profile has an active shallow root zone that extends from the soil surface to a depth of Z_{rz}. The upper boundary of this profile is the soil surface, and the lower boundary is located below the depth of seasonal groundwater level fluctuations within the zone of predominantly vertical flow. A root system distributed along this profile intakes water at a net rate of $ET(t)$. This rate depends on potential evapotranspiration and the root water uptake reduction in accordance with a model characterized by an S-shaped curve (Šimůnek et al., 2008).

4.3.2. Governing equations

The saturated–unsaturated one-dimensional numerical model HYDRUS-1D (Šimůnek et al., 2008) was used to simulate water flow and root water uptake by phreatophytic vegetation (*Populus euphratica* and *Tamarix ramosissima*). The 1-D Richards' equation, which governs one-dimensional unsaturated vertical flow in a homogeneous, isotropic porous medium with a sink term added to simulate the water extraction by roots can be written as follows:

$$\frac{\partial\theta(h)}{\partial t}=\frac{\partial}{\partial z}\left(K(h)\frac{\partial h}{\partial z}\right)+\frac{\partial K(h)}{\partial z}-S(h,z), \tag{9}$$

where $\theta(h)$ is the volumetric water content [$L^3\,L^{-3}$], $K(h)$ is the unsaturated hydraulic conductivity [$L\,T^{-1}$], $S(h)$ is the sink term [$L^3\,L^{-3}\,T^{-1}$], h is the soil water pressure head [L], z is the vertical space coordinate [L], and t is the time [T].

The sink term is specified in terms of the potential uptake rate and the stress factor as follows:

$$S(h)=\alpha(h)S_p(z), \tag{10}$$

where S_p is the potential water uptake rate [$L^3\,L^{-3}\,T^{-1}$], which depends on the root density and the integral of $S_p(z)$ over the root zone is equivalent to potential transpiration, and $\alpha(h)$ is the dimensionless water stress response function ($0\leqslant\alpha(h)\leqslant 1$) that prescribes the reduction in uptake that occurs due to drought stress. For calculating root water uptake, an S-shaped function, which describes the water uptake stress response function $\alpha(h)$ in the HYDRUS-1D using a compensated root water uptake model, was used (van Genuchten, 1987):

$$\alpha(h)=\frac{1}{1+(h/h_{50})^p}, \tag{11}$$

where h_{50} represents the pressure head at which the rate of root water extraction is reduced by 50%, and p is an empirical parameter that determines the steepness of the transition from potential to reduced uptake rates as h decreases. The recommended value of the parameter p is 3 (van Genuchten, 1987). The adaptation of the root to water stress is simulated using a compensation model that includes parameter of critical water stress index for root water uptake (ω) (Šimůnek and Hopmans, 2009).

4.3.3. Numerical modeling

The numerical model consists of a 500-cm-thick soil profile discretized into 1-cm elements. The upper boundary was specified as an atmospheric boundary condition, and the temporal variability values of the precipitation, potential evaporation, and transpiration input data were produced using the special preprocessing code SurfBal 3.60 (Grinevskii and Pozdnyakov, 2010), which calculates surface water balance using meteorological data and leaf area index (LAI) and creates an Atmosph.in input file for use in the HYDRUS-1D. The lower boundary was specified as a constant hydraulic head boundary below an artificial 2-cm semi-permeable confining layer to simulate hydraulic resistance between the water table and the confined aquifer below. The initial hydraulic head in the upper unconfined aquifer was assumed to be equivalent to the constant hydraulic head at the lower boundary. Therefore, the water table in the upper unconfined aquifer will decline due to root water uptake during growing season, while the underlying confined aquifer will serve as an infinite source of groundwater to the overlying unconfined aquifer.

Values of the soil hydraulic parameters were assigned to each of the layers at the two sites, as listed in Table 1. The values of the *van Genuchten* model parameters for the semi-permeable confining layer (silty clay) were the same as those provided in the database of the HYDRUS software (Šimůnek et al., 2008), with the exception of the hydraulic conductivity values (0.01 cm/d). Moreover, the unsaturated hydraulic properties of the sandy gravel layer at site FS1 (depth interval of 0.3–1.7 m) were assumed to be similar to those of the sandy soil. For the sandy soil, the values of the *van Genuchten* parameters were those provided by the HYDRUS-1D database in accordance to the soil catalog (Šimůnek et al., 2008).

The species selected for the simulations were the two dominant phreatophytes, *Tamarix ramosissima* and *Populus euphratica*, which were observed growing at sites FS1 and FS2, respectively. The NDVI analyses conducted at the two field sites indicated that the average

NDVI values during the period of 2010–2012 were 0.132 and 0.196 at sites FS1 and FS2, respectively (Fig. 5). Based on previous studies (Chen et al., 2004; Wang et al., 2003), a representative LAI of 0.2 m^2/m^2 (minimum) to 2.2 m^2/m^2 (maximum) for *Tamarix ramosissima* and 0.2 m^2/m^2 (minimum) to 3.2 m^2/m^2 (maximum) for *Populus euphratica* were used in the simulation. The root distributions of *Tamarix ramosissima* and *Populus euphratica* were fixed during the simulations and were used to weight the water uptake function. The root distribution of *Populus euphratica* was assigned the following normalized function (Zhu et al., 2009):

$$b(z) = \begin{cases} 1/(3L_r), & Z \in (0; 0.3Z_{rz}) \\ 3/L_r, & Z \in (0.3Z_{rz}; 0.5Z_{rz}) \\ 5/(8L_r), & Z \in (0.5Z_{rz}; 0.9Z_{rz}) \\ 1/(2L_r), & Z \in (0.9Z_{rz}; 1.0Z_{rz}) \end{cases}, \quad (12)$$

where Z_{rz} is the depth of the root zone [L], and L_r is the total length of the roots [L]. We assumed that *Tamarix ramosissima* has root distributions that are similar to that of *Populus euphratica*.

4.3.4. Seasonal variation in groundwater ET

The simulations were performed assuming a constant head pressure at the lower 300-cm boundary and using the water uptake reduction parameters of $h_{50} = -950$ cm and $p = 3$ (Grinevskii, 2011; Zhu et al., 2009). The compensated root water uptake model was calibrated using a manual calibration procedure designed to maintain good agreement between the simulated actual root water uptake rates (ET_g simulated) and the estimated ET_g rates obtained using the WTF method (ET_g estimated) during the calculation periods by applying a subset of the root zone depth (Z_{rz}) and the parameter of critical water stress index for root water uptake (ω) (Šimůnek and Hopmans, 2009). Table 3 shows the estimated ET_g and the mean simulated ET_g during the three periods at the two sites. The *RMSE* and *MAE* values for the ET_g values simulated during the three periods at both sites were equivalent to 5–8% of the average ET_g, which indicates the satisfactory performance of the numerical modeling.

Fig. 9 shows the simulated daily ET_g at sites FS1 and FS2 from 2010 to 2012. Clearly, the ET_g at both sites undergoes yearly cycles in which the ET_g is nearly absent during the winter and is at a maximum during the summer. It was noted that approximately 82–86% of the total ET_g occurred during the period from May to August. The average ET_g induced by *Tamarix ramosissima* at site FS1 was approximately 99 mm/yr, whereas the average ET_g due to root water uptake by *Populus euphratica* at site FS2 was approximately 289 mm/yr.

Fig. 10 illustrates the monthly simulated ET_g and measured open water evaporation from the E-601 evaporimeter (E_{601}) during the months of April–October in 2010–2012. It is evident that a strong linear relationship exists between the monthly ET_g and E_{601} at both sites during these periods; the corresponding coefficients of determination are $R^2 = 0.86$ for site FS1 and $R^2 = 0.90$ for site FS2, respectively. At site FS1, ET_g was equivalent to 5% of E_{601} during the growing seasons, whereas ET_g at site FS2 was estimated at approximately of 15% of E_{601} during the same periods.

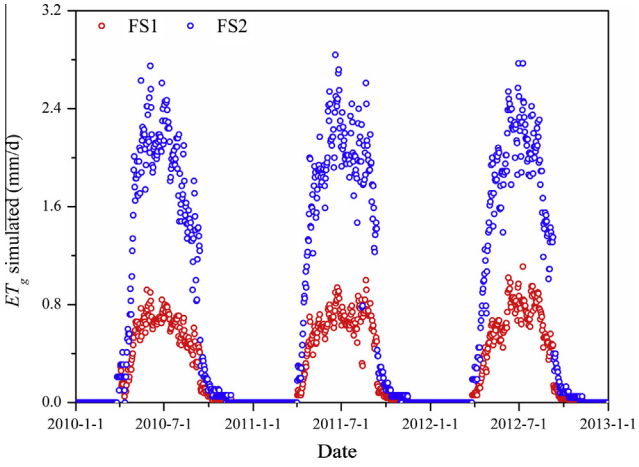

Fig. 9. Daily simulated ET_g at sites FS1 and FS2 from 2010 to 2012.

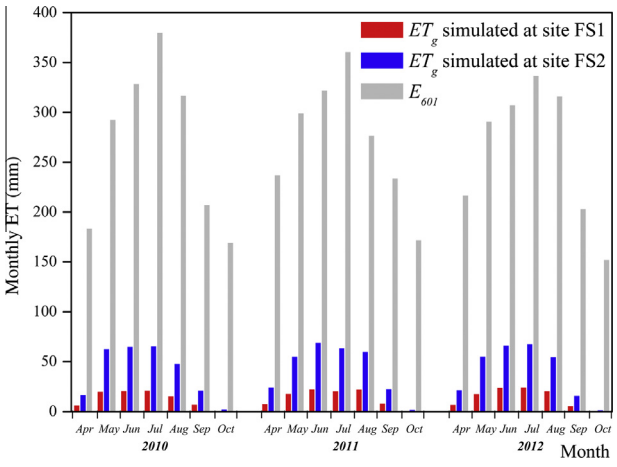

Fig. 10. Monthly simulated ET_g and measured E_{601} for April–October during the period 2010–2012.

5. Discussion

5.1. Scale dependence of the ET estimates

The evapotranspiration rates of *Populus euphratica* and *Tamarix ramosissima* during the growing season (May–September) in this region were recently estimated at tree-level and stand-level scales.

Table 3
Estimated and simulated ET_g and their corresponding goodness-of-fit values.

Period	ET_g estimated (mm/d)	ET_g simulated (mm/d)	*RMSE*[a] (mm/d)	*MAE*[b] (mm/d)
Site FS1 (shrub land)				
I (2010)	0.63	0.62		
II (2011)	0.73	0.69		
III (2012)	0.66	0.74	0.055	0.044
Site FS2 (wood land)				
I (2010)	1.92	1.91		
II (2011)	2.33	2.12		
III (2012)	1.89	1.99	0.133	0.106

[a] Root mean square error, $RMSE = \sqrt{\frac{1}{n}\sum_{i=1}^{n}(x_i - y_i)^2}$.
[b] Mean absolute error, $MAE = \frac{1}{n}\sum_{i=1}^{n}|x_i - y_i|$.

For example, the evapotranspiration rate in a 25-year-old *Populus euphratica* forest with a canopy density of 0.8 (the average height of the *Populus euphratica* forest was 10 m) was determined using sap flux measurements in 2003 (Zhang et al., 2007) and the Bowen ratio-energy balance method in 2005 (Hou et al., 2010). These studies determined that the average evapotranspiration rate of *Populus euphratica* during the growing season was 1.4 mm/d (Zhang et al., 2007) and 3.2 mm/d (Hou et al., 2010). A similar study was conducted by Si et al. (2005) to quantify the evapotranspiration of *Tamarix ramosissima* (the canopy density was 0.7, and the average height was 2 m) using the Bowen ratio method during the growing season in 2003. The total evapotranspiration of *Tamarix ramosissima* was approximately 248 mm, with an average evapotranspiration rate of 1.6 mm/d (Si et al., 2005).

A comparison of the results obtained in this study and those of the aforementioned studies indicates that the ET_g rates estimated using the WTF method at both the *Populus euphratica* and *Tamarix ramosissima* sites are lower than the values determined using the Bowen ratio method but higher than the value obtained using the sap flux method. Clearly, there were differences between the climatic and hydrological conditions and vegetation parameters at the study sites; however, the differences in the estimated evapotranspiration rates observed at each site are likely related to the use of different quantitative methods. Numerous studies have reported that ET_g estimates based on WTF approaches tend to be significantly different from sap flow measurements (Engel et al., 2005), eddy covariance measurements (Martinet et al., 2009; Soylu et al., 2012), and lysimeter measurements (Fahle and Dietrich, 2014). As concluded by Dawson (1996), variations in the estimates of plant evapotranspiration using various techniques (e.g., sap flow, Bowen ratio, and water balance method) are directly associated with variations in the measurements of water loss at various scales, such as from leaves to stands and from stands to landscapes. Earlier studies have indicated that estimates of ET_g using the WTF method represent ET_g across areas measuring several hundreds (Delin et al., 2007) if not thousands (Healy, 2010) of square meters.

5.2. Limitations of applying the WTF method

Applying the WTF method based on seasonal declines in the groundwater level may involve a high degree of uncertainty in the ET_g estimates, which are associated with time-dependent lateral flow rates. As shown in Fig. 11, ET_g exhibited a negative linear relationship with the lateral flow rates at both field sites. During the three calculation periods encompassing 2010–2012, the changes in the lateral flow rates of ±25% caused the estimated ET_g to vary by approximately ∓47% at site FS1 and ∓18% at site FS2 (Fig. 11). The described method is based on an assumption that the lateral flow is independent from the local recharge/discharge processes and changes in the lateral flow rates in the riparian zone are negligible during the selected calculation periods. However, as noted previously (e.g., Gribovszki et al., 2008; Troxell, 1936), the lateral flow rate clearly varies, even over the course of a day, due to changes in the hydraulic gradients that are induced by the direct uptake of groundwater by roots. Therefore, the assumption of a constant lateral flow rate during the growing season can introduce considerable uncertainties in ET_g estimations using the WTF approach. In addition, the pattern and amplitude of water table fluctuations are highly dependent on the monitoring well locations within riparian areas (Loheide, 2008), which may vary from the edges to the center of a vegetated riparian zone (Butler et al., 2007). The spatial variability in water table fluctuations is likely a result of spatial heterogeneity in the permeability and specific yield of the aquifer in which the monitoring wells are installed (Rosenberry and Winter, 1997; Martinet et al., 2009) and may be partially caused by spatial variability in the species composition and vegetation structure. Therefore, we question whether estimates of ET_g based on the hydrographs from single monitoring wells can represent the average water uptake by plants in a riparian zone.

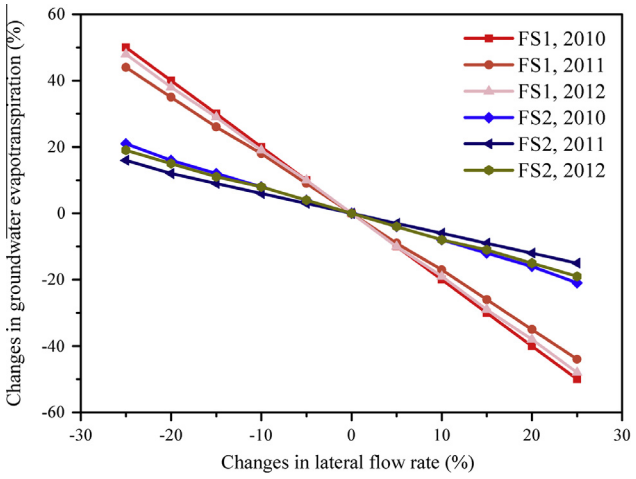

Fig. 11. Sensitivity analysis of groundwater evapotranspiration to changes in the lateral flow rate at field sites FS1 and FS2.

One aspect that reduces the degree of uncertainty associated with time-dependent lateral flow rates, which is also defined as net inflow rate by White (1932), is to develop different "empirical" approaches (Gribovszki et al., 2008) or techniques for quantifying this parameter. Various time spans have been recommended for determining the net inflow rate at different field sites when using the diurnal WTF method (e.g., Loheide, 2008; Miller et al., 2010; Rushton, 1996; White, 1932). Fahle and Dietrich (2014) also demonstrated that estimating the daily net inflow rate can be improved by using longer time spans and estimating ET_g can be enhanced by applying two-night averaged net inflow rates. Recently, Loheide (2008) introduced detrending procedures in the analysis of groundwater level time series for determining a reliable net inflow rate and ET_g. Furthermore, the "Fourier method" (Soylu et al., 2012) and "statistical approach" (Wang and Pozdniakov, 2014), which are both based on the relationship between ET_g and general characteristics of diurnal detrended groundwater level fluctuations, have been developed to estimate ET_g by avoiding the direct determination of the net inflow rate. Another important aspect that minimizes the high level of uncertainty that is related to the time-dependent lateral flow rate is the development of a "hydraulic" approach (Gribovszki et al., 2008), which involves implementing a reliable groundwater monitoring network that should be designed along flow paths from recharge to discharge areas. The "hydraulic" approach is particularly important for reducing the subjectivity that is inherent in estimates of the transient lateral flow rate and enhancing the performance of the WTF method in ET_g estimations that are based on the diurnal and seasonal fluctuations in the groundwater level.

6. Conclusions

Our analysis of groundwater level data, soil profiles, and vegetation characteristics at two typical phreatophyte-dominated sites (*Tamarix ramosissima* and *Populus euphratica*) located in hyper-arid desert environments in northwestern China indicates that groundwater evapotranspiration is an important factor that controls hydrologic processes in arid riparian areas. In these regions, the

presence of diurnal water table fluctuations during the summer may be attributed to groundwater evapotranspiration due to direct root water uptake by plants. The overall characteristics of the diurnal water table fluctuation amplitude, i.e., the standard deviation of the detrended diurnal water table fluctuations, can serve as an important diagnostic indicator of groundwater evapotranspiration.

Seasonal declines in the groundwater tables can be used to quantify groundwater evapotranspiration rates, and the accuracy and precision of the ET_g quantification depend largely on reliable estimates of the lateral groundwater flow rates, the redistribution of water within riparian aquifers during periods of river flow (Wondzell et al., 2010), and the specific yields (Healy and Cook, 2002). In this study, a steady water table decline during the growing season was observed at both of the phreatophyte-dominated sites. Using the WTF method, the average ET_g rate during the summer months (June–August) of 2010–2012 was estimated to be 0.63–0.73 mm/d at the site dominated by *Tamarix ramosissima* and 1.89–2.33 mm/d at the site dominated by *Populus euphratica*, depending on climatic conditions, vegetation status, and depth to water table.

A 1-D root water uptake model was employed to help develop an understanding of the temporal variations in groundwater evapotranspiration and to support the WTF method results. The simulated ET_g varied seasonally at both sites, and these trends were primarily a function of the potential evaporation rates. During the period of April–October, ET_g was equivalent to 5% of the open water evaporation measured using the E-601 pan method (E_{601}) at the *Tamarix ramosissima* site, whereas ET_g was equivalent to approximately 15% of E_{601} at the *Populus euphratica* site.

Clearly, estimation of ET_g based on the WTF method may be considered the simplest, easiest, and least expensive technique available, but equally important, the method involves a number of sources of uncertainty (Soylu et al., 2012). In particular, the proposed method is based on the assumption that the lateral flow is independent of local evapotranspiration processes and that the lateral flow rates remain constant during the calculated periods, which is oversimplified compared to real-world scenarios in which the lateral flow rate is highly time-dependent and can vary over the course of a day. Because of the time-dependent lateral flow rate, spatial variations in the patterns of groundwater dynamics and specific yields in riparian corridors, it is particularly important to develop an effective network of monitoring wells for estimating groundwater evapotranspiration rather than using a single monitoring well (Martinet et al., 2009). In addition, a reliable quantification of riparian evapotranspiration requires a comprehensive investigation that combines the WTF method with traditional approaches, such as the Bowen ratio method and eddy covariance method.

Acknowledgments

This research was supported by grants from the National Natural Science Foundation of China (Nos. 41271049, 41301025, and 41371059), the NSFC-RFBR Program 2013–2014 (Nos. 41311120068 and 13-05-91161), the Visiting Professorship for Senior International Scientists, Chinese Academy of Sciences (No. 2012T1Z0037), and the Russian Federation Basic Research Foundation (No. 13-05-91161-Г_ФЕН_а). We would like to thank Yongliang Xu, Zhiyong Wang, and Dandan Wang for their participation in the fieldwork. The authors gratefully acknowledge the Editor, Corrado Corradini, the anonymous associate editor, and the anonymous reviewers for their valuable comments and suggestions that led to substantial improvements in the manuscript. The first author would also like to thank the China Scholarship Council (No. 201304910063) for its additional support of this work.

References

Akaike, H., 1980. Seasonal adjustment by a Bayesian modeling. J. Time Ser. Anal. 1 (1), 1–13.
Alley, W.M., Healy, R.W., LaBaugh, J.W., Reilly, T.E., 2002. Flow and storage in groundwater systems. Science 296 (5575), 1985–1990.
Butler, J.J., Kluitenberg, G.J., Whittemore, D.O., Loheide II, S.P., Jin, W., Billinger, M.A., Zhan, X., 2007. A field investigation of phreatophyte-induced fluctuations in the water table. Water Resour. Res. 43 (2), W02404.
Carlson Mazur, M.L., Wiley, M.J., Wilcox, D.A., 2014. Estimating evapotranspiration and groundwater flow from water-table fluctuations for a general wetland scenario. Ecohydrology 7 (2), 378–390.
Chen, R., Kang, E., Zhao, W., Zhang, Z., Yang, J., Zhang, J., 2004. Trees transpiration response to meteorological variables in arid regions of Northwest China. Acta Ecol. Sin. (03), 477–485 (in Chinese with English abstract).
Chen, X., Song, J., Wang, W., 2010. Spatial variability of specific yield and vertical hydraulic conductivity in a highly permeable alluvial aquifer. J. Hydrol. 388 (3–4), 379–388.
Cheng, D.-H., Li, Y., Chen, X., Wang, W., Hou, G., Wang, C., 2013. Estimation of groundwater evapotranspiration using diurnal water table fluctuations in the Mu Us Desert, northern China. J. Hydrol. 490, 106–113.
Cleverly, J.R., Dahm, C.N., Thibault, J.R., McDonnell, D.E., Allred Coonrod, J.E., 2006. Riparian ecohydrology: regulation of water flux from the ground to the atmosphere in the Middle Rio Grande, New Mexico. Hydrol. Process. 20 (15), 3207–3225.
Cooper, D.J., Sanderson, J.S., Stannard, D.I., Groeneveld, D.P., 2006. Effects of long-term water table drawdown on evapotranspiration and vegetation in an arid region phreatophyte community. J. Hydrol. 325 (1–4), 21–34.
Crosbie, R.S., Binning, P., Kalma, J.D., 2005. A time series approach to inferring groundwater recharge using the water table fluctuation method. Water Resour. Res. 41 (1), W01008.
Dawson, T.E., 1996. Determining water use by trees and forests from isotopic, energy balance and transpiration analyses: the roles of tree size and hydraulic lift. Tree Physiol. 16 (1–2), 263–272.
Delin, G.N., Healy, R.W., Lorenz, D.L., Nimmo, J.R., 2007. Comparison of local- to regional-scale estimates of ground-water recharge in Minnesota, USA. J. Hydrol. 334 (1–2), 231–249.
Devitt, D.A., Fenstermaker, L.F., Young, M.H., Conrad, B., Baghzouz, M., Bird, B.M., 2011. Evapotranspiration of mixed shrub communities in phreatophytic zones of the Great Basin region of Nevada (USA). Ecohydrology 4 (6), 807–822.
Drexler, J.Z., Snyder, R.L., Spano, D., Paw U, K.T., 2004. A review of models and micrometeorological methods used to estimate wetland evapotranspiration. Hydrol. Process. 18 (11), 2071–2101.
Duke, H., 1972. Capillary properties of soils – influence upon specific yield. Trans. Am. Soc. Agr. Eng. 15, 688–691.
Engel, V., Jobbágy, E.G., Stieglitz, M., Williams, M., Jackson, R.B., 2005. Hydrological consequences of *Eucalyptus* afforestation in the Argentine Pampas. Water Resour. Res. 41 (10), W10409.
Fahle, M., Dietrich, O., 2014. Estimation of evapotranspiration using diurnal groundwater level fluctuations: comparison of different approaches with groundwater lysimeter data. Water Resour. Res. 50 (1), 273–286.
Freeman, L.A., Carpenter, M.C., Rosenberry, D.O., Rousseau, J.P., Unger, R., McLean, J.S., 2004. Use of submersible pressure transducers in water-resources investigations. In: U.S. Geol. Surv. Tech. Water Resour. Invest. U.S. Department of the Interior, U.S. Geological Survey, vol. 8–A3.
Goodrich, D.C., Scott, R., Qi, J., Goff, B., Unkrich, C.L., Moran, M.S., Williams, D., Schaeffer, S., Snyder, K., MacNish, R., Maddockb, T., Poole, D., Chehbounif, A., Cooperg, D.I., Eichingerh, W.E., Shuttleworthb, W.J., Kerri, Y., Marsetta, R., Ni, W., 2000. Seasonal estimates of riparian evapotranspiration using remote and in situ measurements. Agric. For. Meteorol. 105 (1–3), 281–309.
Gou, S., Miller, G., 2014. A groundwater–soil–plant–atmosphere continuum approach for modelling water stress, uptake, and hydraulic redistribution in phreatophytic vegetation. Ecohydrology 7 (3), 1029–1041.
Gribovszki, Z., Kalicz, P., Szilágyi, J., Kucsara, M., 2008. Riparian zone evapotranspiration estimation from diurnal groundwater level fluctuations. J. Hydrol. 349 (1–2), 6–17.
Gribovszki, Z., Szilágyi, J., Kalicz, P., 2010. Diurnal fluctuations in shallow groundwater levels and streamflow rates and their interpretation – a review. J. Hydrol. 385 (1–4), 371–383.
Gribovszki, Z., Kalicz, P., Szilágyi, J., 2013. Does the accuracy of fine-scale water level measurements by vented pressure transducers permit for diurnal evapotranspiration estimation? J. Hydrol. 488, 166–169.
Grinevskii, S.O., 2011. Modeling root water uptake when calculating unsaturated flow in the vadose zone and groundwater recharge. Mosc. Univ. Geol. Bull. 66 (3), 189–201.
Grinevskii, S.O., Pozdnyakov, S.P., 2010. Principles of regional estimation of infiltration groundwater recharge based on geohydrological models. Water Resour. 37 (5), 638–652.
Healy, R.W., 2010. Estimating Groundwater Recharge. Cambridge University Press.
Healy, R.W., Cook, P.G., 2002. Using groundwater levels to estimate recharge. Hydrogeol. J. 10 (1), 91–109.
Hou, L.G., Xiao, H.L., Si, J.H., Xiao, S.C., Zhou, M.X., Yang, Y.G., 2010. Evapotranspiration and crop coefficient of *Populus euphratica Oliv* forest during the growing season in the extreme arid region northwest China. Agric. Water Manage. 97 (2), 351–356.

Huete, A., Didan, K., Miura, T., Rodriguez, E.P., Gao, X., Ferreira, L.G., 2002. Overview of the radiometric and biophysical performance of the MODIS vegetation indices. Remote Sens. Environ. 83 (1–2), 195–213.
Jarlan, L., Mangiarotti, S., Mougin, E., Mazzega, P., Hiernaux, P., Le Dantec, V., 2008. Assimilation of SPOT/VEGETATION NDVI data into a sahelian vegetation dynamics model. Remote Sens. Environ. 112 (4), 1381–1394.
Johnson, A.I., 1967. Specific Yield – Compilation of Specific Yields for Various Materials. USGS Water Supply Paper: 1662-D. 74 pp.
Jolly, I.D., McEwan, K.L., Holland, K.L., 2008. A review of groundwater–surface water interactions in arid/semi-arid wetlands and the consequences of salinity for wetland ecology. Ecohydrology 1 (1), 43–58.
Lautz, L., 2008. Estimating groundwater evapotranspiration rates using diurnal water-table fluctuations in a semi-arid riparian zone. Hydrogeol. J. 16 (3), 483–497.
Loheide II, S.P., 2008. A method for estimating subdaily evapotranspiration of shallow groundwater using diurnal water table fluctuations. Ecohydrology 1 (1), 59–66.
Loheide II, S.P., Butler Jr., J.J., Gorelick, S.M., 2005. Estimation of groundwater consumption by phreatophytes using diurnal water table fluctuations: a saturated–unsaturated flow assessment. Water Resour. Res. 41 (7), W07030.
Mangiarotti, S., Mazzega, P., Hiernaux, P., Mougin, E., 2012. Predictability of vegetation cycles over the semi-arid region of Gourma (Mali) from forecasts of AVHRR-NDVI signals. Remote Sens. Environ. 123, 246–257.
Martinet, M.C., Vivoni, E.R., Cleverly, J.R., Thibault, J.R., Schuetz, J.F., Dahm, C.N., 2009. On groundwater fluctuations, evapotranspiration, and understory removal in riparian corridors. Water Resour. Res. 45 (5), W05425.
McGwire, K., Minor, T., Fenstermaker, L., 2000. Hyperspectral mixture modeling for quantifying sparse vegetation cover in arid environments. Remote Sens. Environ. 72 (3), 360–374.
Meyboom, P., 1965. Three observations on streamflow depletion by phreatophytes. J. Hydrol. 2 (3), 248–261.
Miller, G.R., Chen, X., Rubin, Y., Ma, S., Baldocchi, D.D., 2010. Groundwater uptake by woody vegetation in a semiarid oak savanna. Water Resour. Res. 46 (10), W10503.
Min, L., Yu, J., Liu, C., Zhu, J., Wang, P., 2013. The spatial variability of streambed vertical hydraulic conductivity in an intermittent river, northwestern China. Environ. Earth Sci. 69 (3), 873–883.
Nachabe, M.H., 2002. Analytical expressions for transient specific yield and shallow water table drainage. Water Resour. Res. 38 (10), 1193.
Naumburg, E., Mata-gonzalez, R., Hunter, R.G., McLendon, T., Martin, D.W., 2005. Phreatophytic vegetation and groundwater fluctuations: a review of current research and application of ecosystem response modeling with an emphasis on Great Basin vegetation. Environ. Manage. 35 (6), 726–740.
Newman, B.D., Wilcox, B.P., Archer, S.R., Breshears, D.D., Dahm, C.N., Duffy, C.J., McDowell, N.G., Phillips, F.M., Scanlon, B.R., Vivoni, E.R., 2006. Ecohydrology of water-limited environments: a scientific vision. Water Resour. Res. 42 (6), W06302.
Nichols, W.D., 1994. Groundwater discharge by phreatophyte shrubs in the Great Basin as related to depth to groundwater. Water Resour. Res. 30 (12), 3265–3274.
Nimmo, J.R., Horowitz, C., Mitchell, L., 2014. Discrete-storm water-table fluctuation method to estimate episodic recharge. Groundwater. http://dx.doi.org/10.1111/gwat.12177.
Orellana, F., Verma, P., Loheide II, S.P., Daly, E., 2012. Monitoring and modeling water-vegetation interactions in groundwater-dependent ecosystems. Rev. Geophys. 50 (3), RG3003.
Post, V.A., Asmuth, J., 2013. Review: hydraulic head measurements—new technologies, classic pitfalls. Hydrogeol. J. 21 (4), 737–750.
Qin, D., Zhao, Z., Han, L., Qian, Y., Ou, L., Wu, Z., Wang, M., 2012. Determination of groundwater recharge regime and flowpath in the Lower Heihe River Basin in an arid area of Northwest China by using environmental tracers: implications for vegetation degradation in the Ejina Oasis. Appl. Geochem. 27 (6), 1133–1145.
Ridolfi, L., D'Odorico, P., Laio, F., 2007. Vegetation dynamics induced by phreatophyte–aquifer interactions. J. Theor. Biol. 248 (2), 301–310.
Rosenberry, D.O., Winter, T.C., 1997. Dynamics of water-table fluctuations in an upland between two prairie-pothole wetlands in North Dakota. J. Hydrol. 191 (1–4), 266–289.
Rushton, B., 1996. Hydrologic budget for a freshwater marsh in Florida. J. Am. Water Resour. Assoc. 32 (1), 13–21.
Shah, N., Ross, M., 2009. Variability in specific yield under shallow water table conditions. J. Hydrol. Eng. 14 (12), 1290–1298.
Shah, N., Nachabe, M., Ross, M., 2007. Extinction depth and evapotranspiration from ground water under selected land covers. Ground Water 45 (3), 329–338.
Shtengelov, R.S., 2009. REGIM_3: Program of Data Processing in Experimental Filtration Observations (National Registration Number 2009611414). Department of Hydrogeology, Moscow State University, Moscow.
Si, J.H., Feng, Q., Zhang, X.Y., Liu, W., Su, Y.H., Zhang, Y.W., 2005. Growing season evapotranspiration from *Tamarix ramosissima* stands under extreme arid conditions in northwest China. Environ. Geol. 48 (7), 861–870.
Si, J., Feng, Q., Cao, S., Yu, T., Zhao, C., 2014. Water use sources of desert riparian *Populus euphratica* forests. Environ. Monit. Assess. 186 (9), 5469–5477.
Šimůnek, J., Hopmans, J.W., 2009. Modeling compensated root water and nutrient uptake. Ecol. Model. 220 (4), 505–521.
Šimůnek, J., van Genuchten, M.T., Šejna, M., 2008. Development and applications of the HYDRUS and STANMOD software packages and related codes. Vadose Zone J. 7 (2), 587–600.
Sophocleous, M.A., 1991. Combining the soilwater balance and water-level fluctuation methods to estimate natural groundwater recharge – practical aspects. J. Hydrol. 124 (3–4), 229–241.
Soylu, M.E., Lenters, J.D., Istanbulluoglu, E., Loheide II, S.P., 2012. On evapotranspiration and shallow groundwater fluctuations: a Fourier-based improvement to the White method. Water Resour. Res. 48 (6), W06506.
Toll, N.J., Rasmussen, T.C., 2007. Removal of barometric pressure effects and earth tides from observed water levels. Ground Water 45 (1), 101–105.
Törnros, T., Menzel, L., 2014. Addressing drought conditions under current and future climates in the Jordan River region. Hydrol. Earth Syst. Sci. 18 (1), 305–318.
Troxell, H., 1936. The diurnal fluctuation in the ground-water and flow of the Santa Ana River and its meaning. Trans. Am. Geophys. Union 17 (4), 496–504.
van Genuchten, M.T., 1987. A Numerical Model for Water and Solute Movement in and Below the Root Zone, Research Report No. 121. U.S. Salinity Laboratory, USDA, ARS, Riverside, California.
van Genuchten, M.T., Leij, F.J., Yates, S.R., 1991. The RETC Code for Quantifying the Hydraulic Functions of Unsaturated Soils. Version 1.0. EPA Report 600/2-91/065, U.S. Salinity Laboratory, USDA, ARS, Riverside, California.
Varni, M., Comas, R., Weinzettel, P., Dietrich, S., 2013. Application of the water table fluctuation method to characterize groundwater recharge in the Pampa plain, Argentina. Hydrol. Sci. J. 58 (7), 1445–1455.
Wang, K., Dickinson, R.E., 2012. A review of global terrestrial evapotranspiration: observation, modeling, climatology, and climatic variability. Rev. Geophys. 50 (2), RG2005.
Wang, P., Pozdniakov, S.P., 2014. A statistical approach to estimating evapotranspiration from diurnal groundwater level fluctuations. Water Resour. Res. 50 (3), 2276–2292.
Wang, L., Zhang, Q., Yin, J., 2003. Study on the growth pattern and bio-productivity of the *Populus euphratica* forest stand in Ejina. J. Arid Land Resour. Environ. (02), 94–99 (in Chinese with English abstract).
Wang, P., Yu, J., Zhang, Y., Fu, G., Min, L., Ao, F., 2011a. Impacts of environmental flow controls on the water table and groundwater chemistry in the Ejina Delta, northwestern China. Environ. Earth Sci. 64 (1), 15–24.
Wang, P., Zhang, Y., Yu, J., Fu, G., Ao, F., 2011b. Vegetation dynamics induced by groundwater fluctuations in the lower Heihe River Basin, northwestern China. J. Plant Ecol. 4 (1–2), 77–90.
Wang, P., Yu, J., Zhang, Y., Liu, C., 2013. Groundwater recharge and hydrogeochemical evolution in the Ejina Basin, northwest China. J. Hydrol. 476, 72–86.
Wang, P., Yu, J., Pozdniakov, S.P., Grinevsky, S.O., Liu, C., 2014. Shallow groundwater dynamics and its driving forces in extremely arid areas: a case study of the lower Heihe River in northwestern China. Hydrol. Process. 28 (3), 1539–1553.
Weeks, E.P., Sorey, M.L., 1973. Use of Finite-difference Arrays of Observation Wells to Estimate Evapotranspiration from Ground Water in the Arkansas River Valley, Colorado, US Geological Survey Water Supply Paper 2029-C.
Wen, X., Wu, Y., Su, J., Zhang, Y., Liu, F., 2005. Hydrochemical characteristics and salinity of groundwater in the Ejina Basin, Northwestern China. Environ. Geol. 48 (6), 665–675.
White, W.N., 1932. A Method of Estimating Ground-water Supplies Based on Discharge by Plants and Evaporation from Soil: Results of Investigation in Escalante Valley, Utah, Washington DC, US Geological Survey. Water Supply Paper 659-A, United States Department of the Interior.
Woessner, W.W., 2000. Stream and fluvial plain ground water interactions: rescaling hydrogeologic thought. Ground Water 38 (3), 423–429.
Wondzell, S.M., Gooseff, M.N., McGlynn, B.L., 2010. An analysis of alternative conceptual models relating hyporheic exchange flow to diel fluctuations in discharge during baseflow recession. Hydrol. Process. 24 (6), 686–694.
Xie, Q., 1980. Regional Hydrogeological Survey Report of the People's Republic of China (1:200 000): Ejina K-47-[24] [R], Jiuquan (in Chinese).
Yin, L., Zhou, Y., Ge, S., Wen, D., Zhang, E., Dong, J., 2013. Comparison and modification of methods for estimating evapotranspiration using diurnal groundwater level fluctuations in arid and semiarid regions. J. Hydrol. 496, 9–16.
Yuan, G., Zhang, P., Shao, M.-A., Luo, Y., Zhu, X., 2014. Energy and water exchanges over a riparian *Tamarix spp.* stand in the lower Tarim River basin under a hyper-arid climate. Agric. For. Meteorol. 194, 144–154.
Zhang, X., Kang, E., Zhou, M., 2007. Evaluation of the sap flow using heat pulse method to determine transpiration of the *Populus euphratica* canopy. Front. Forest. China 2 (3), 323–328.
Zhang, Y., Yu, J., Wang, P., Fu, G., 2011. Vegetation responses to integrated water management in the Ejina basin, northwest China. Hydrol. Process. 25 (22), 3448–3461.
Zhu, Y., Ren, L., Skaggs, T.H., Lu, H., Yu, Z., Wu, Y., Fang, X., 2009. Simulation of *Populus euphratica* root uptake of groundwater in an arid woodland of the Ejina Basin, China. Hydrol. Process. 23 (17), 2460–2469.
Zhu, J., Young, M., Healey, J., Jasoni, R., Osterberg, J., 2011. Interference of river level changes on riparian zone evapotranspiration estimates from diurnal groundwater level fluctuations. J. Hydrol. 403 (3–4), 381–389.
Zhu, J., Yu, J., Wang, P., Zhang, Y., Yu, Q., 2012. Interpreting the groundwater attributes influencing the distribution patterns of groundwater-dependent vegetation in northwestern China. Ecohydrology 5 (5), 628–636.